ANNUAL REVIEWS

*Annual Review of Biophysics*

# The Sliding Filament Theory Since Andrew Huxley: Multiscale and Multidisciplinary Muscle Research

Joseph D. Powers,[1,*] Sage A. Malingen,[2,*] Michael Regnier,[3,4] and Thomas L. Daniel[2,3,4]

[1]Department of Bioengineering, University of California San Diego, La Jolla, California 92093, USA

[2]Department of Biology, University of Washington, Seattle, Washington 98195, USA; email: danielt@uw.edu

[3]Department of Bioengineering, University of Washington, Seattle, Washington 98185, USA

[4]Center for Translational Muscle Research, University of Washington, Seattle, Washington 98185, USA



Annu. Rev. Biophys. 2021. 50:373–400

First published as a Review in Advance on February 26, 2021

The *Annual Review of Biophysics* is online at biophys.annualreviews.org

https://doi.org/10.1146/annurev-biophys-110320-062613



*These authors contributed equally to this review.

## Keywords

skeletal muscle, cardiac muscle, sarcomere, myofilament, myosin

## Abstract

Two groundbreaking papers published in 1954 laid out the theory of the mechanism of muscle contraction based on force-generating interactions between myofilaments in the sarcomere that cause filaments to slide past one another during muscle contraction. The succeeding decades of research in muscle physiology have revealed a unifying interest: to understand the multiscale processes—from atom to organ—that govern muscle function. Such an understanding would have profound consequences for a vast array of applications, from developing new biomimetic technologies to treating heart disease. However, connecting structural and functional properties that are relevant at one spatiotemporal scale to those that are relevant at other scales remains a great challenge. Through a lens of multiscale dynamics, we review in this article current and historical research in muscle physiology sparked by the sliding filament theory.

## Contents


1. INTRODUCTION AND HISTORY ..... 374
2. THE MOLECULAR DRIVER OF FILAMENT SLIDING: SINGLE MYOSIN STRUCTURE, KINETICS, AND MECHANICS ..... 377
   - 2.1. Single-Myosin Protein Structure and the ATPase Cycle ..... 377
   - 2.2. Mechanics and Dynamics of Myosin Motors During Contraction ..... 378
   - 2.3. Structure–Function Relationships of Myosin from Pathological and Therapeutic Perspectives ..... 379
3. THE FILAMENTS THAT SLIDE, PULL, AND STRETCH: MYOFILAMENT STRUCTURE, MECHANICS, AND REGULATION ..... 379
   - 3.1. Thin Filament Structure, Mechanics, and Regulation of Contraction ..... 380
   - 3.2. Thick Filament Structure and Composition ..... 381
   - 3.3. Thick Filament–Based Regulation of Contraction ..... 382
   - 3.4. Titin Structure and Mechanics ..... 383
   - 3.5. Titin-Based Regulation of Contraction ..... 384
4. A MICROSCALE MACHINE OF SLIDING FILAMENTS: SARCOMERE STRUCTURE, ORGANIZATION, MECHANICS, AND DYNAMICS ..... 385
   - 4.1. Structure and Organization of the Lattice ..... 385
   - 4.2. Radial Sarcomere Dynamics and Interfilament Regulatory Mechanisms ..... 387
   - 4.3. Axial Sarcomere Dynamics and Interfilament Regulatory Mechanisms ..... 388
   - 4.4. The Ends of the Sarcomere: Z-Disks and Myotendinous Junctions ..... 389
   - 4.5. Efficiency Is an Emergent Property of Multiscale Interactions ..... 389
5. IDEAS FOR THE FUTURE AND THE MULTISCALE PROBLEM ..... 390


## 1. INTRODUCTION AND HISTORY

Two papers published simultaneously in 1954 (71, 77) independently showed that striated muscle shortens as a result of the sliding between two sets of filaments containing the proteins myosin and actin. Thus was born the sliding filament hypothesis. There has been a series of impressive and informative reviews of the history and basis of the sliding filament theory of muscle contraction (e.g., 21, 74, 164, 179). Rather than attempting an expansion on those superb perspectives, we focus in this review on the central idea that muscle contraction is the output of a dynamical system spanning spatial and temporal scales from nanometers and microseconds to meters and minutes, integrating biochemical and mechanical regulation across scales.

Striated muscle's highly structured, nearly crystalline organization sets it apart from other biological systems (**Figure 1**). Single muscle cells are portioned into subcellular elements (myofibrils) that are formed from a series of axially arranged sarcomeres, each consisting of interdigitating systems of axial filaments—the thick and thin filaments. Thin filaments, extending from Z-disks, contain a double-helical strand of actin monomers along with troponin–tropomyosin complexes that are involved in the regulation of contraction. The myosin molecular motors constitute the bulk of the thick filaments and extend radially in the form of a three-start helix.

Supporting evidence for the sliding filament hypothesis was established in a series of papers that melded experimental and theoretical studies of muscle contraction. First, early polarized light (73) and electron microscopy (EM) (77) evidence pointed to the structural overlap of thick and thin filaments, suggesting the idea that the force generation increases with greater filament overlap, a

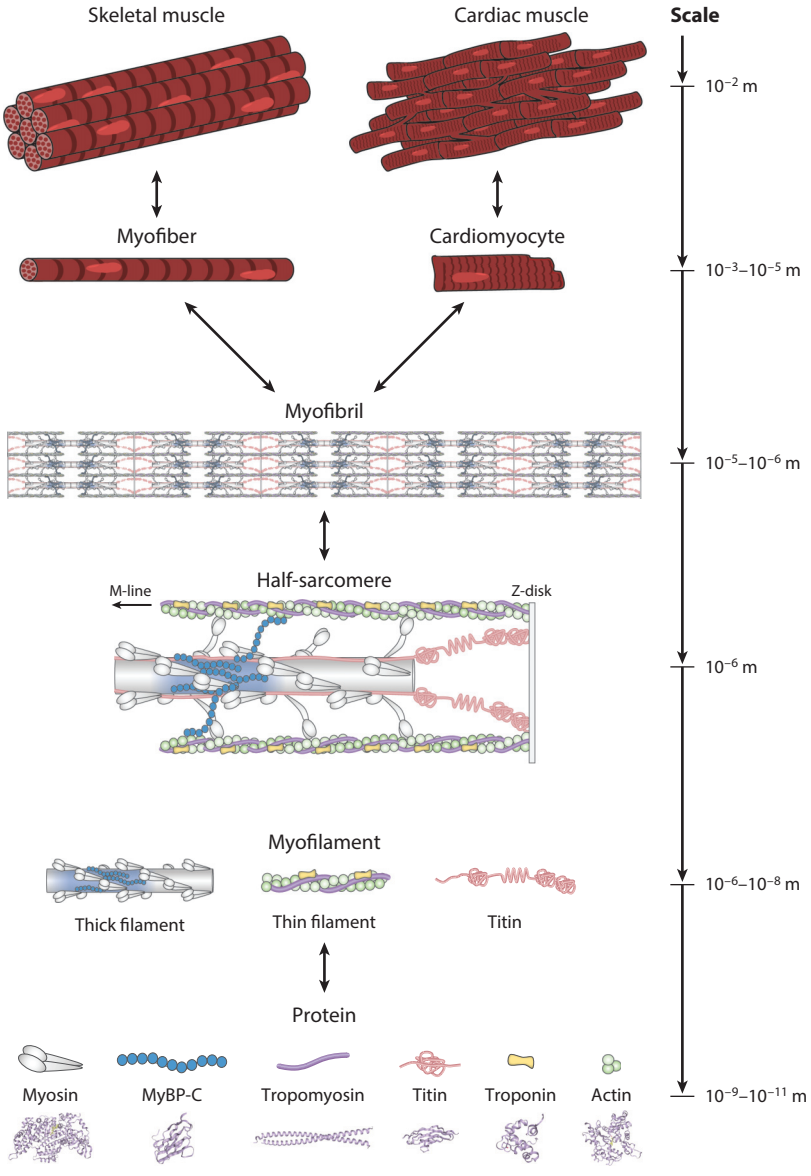


**Figure 1**

An illustration of striated muscle across spatial scales. Generally, skeletal and cardiac muscles are made up of myofibers and cardiomyocytes (respectively) that span tens of microns to tens of millimeters. The subcellular contractile organelle, the myofibril, is structurally similar in myofibers and cardiomyocytes, and its size is on the order of microns. The myofibril is composed of many serially linked sarcomeres (the half-sarcomere is shown for simplicity), each approximately 2–3 microns long. The three main myofilaments that comprise the sarcomere, the thick filament, the thin filament, and titin, are tens to thousands of nanometers in length. The main constituent proteins of the myofilaments are myosin (*gray*), myosin-binding protein C (MyBP-C) (*blue*), tropomyosin (*purple*), titin (*pink*), the troponin complex (*yellow*), and actin (*green*). The structural and functional properties of each spatial scale are highlighted throughout this review, from single-protein to cellular-level function. The atomic representations of each protein or protein subunit from the Protein Data Bank are as follows: myosin, 4DB1; MyBP-C, 2K1M; tropomyosin, 1IC2; titin immunoglobulin domain, 1G1C; troponin, 1MXL; actin, 2ZWH.

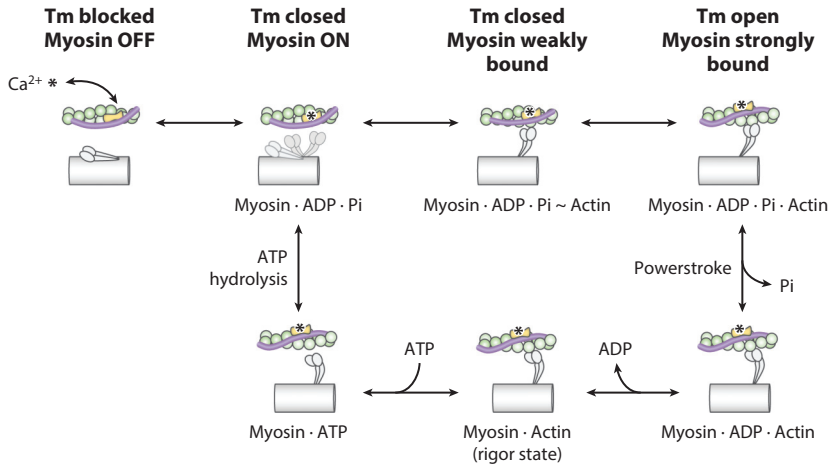


**Figure 2**

The chemomechanical cycle of myosin motors in the sarcomere. When $Ca^{2+}$ is unbound from troponin (*top left*) on the thin filament, tropomyosin (Tm) is in the blocked state, sterically blocking myosin-binding sites on F-actin. Myosin is in a resting conformation, folded onto the thick filament backbone. Upon $Ca^{2+}$ binding to troponin, allosteric interactions within the troponin complex cause azimuthal displacement of Tm along F-actin, allowing Tm to reversibly occupy a closed state. This closed state partially exposes myosin-binding sites on F-actin, permitting weak actomyosin interaction. Myosin is loaded with its energy-bearing hydrolysis products, ADP and inorganic phosphate (Pi). In a process facilitated by multiple intra- and interfilament cooperative activation mechanisms (e.g., nearest-neighbor thin filament activation via Tm, myosin–actin–tropomyosin interactions), Tm is further displaced to an open state that permits strong myosin binding. The powerstroke (or working stroke) occurs when myosin undergoes a conformational change while maintaining its strong interaction with actin, which results in force production along and between the thick and thin filaments. ADP is released postpowerstroke, producing a rigor state until ATP binds to the nucleotide-binding pocket of myosin. With ATP bound, the affinity of myosin for actin is reduced, and myosin dissociates from actin. ATP is then hydrolyzed again, priming myosin for another strong, force-producing interaction with actin.

hypothesis that was tested in the classic studies of length–tension relationships first established by Gordon and colleagues (47) in 1966.

With the goal of understanding the fundamental molecular mechanisms underlying cross-bridge force generation, Huxley established the two- and three-state models of myosin motor mechanics. These models formed a hypothesis that was tested in another landmark paper by Huxley & Simmons (72) in 1971. Their goal was to probe cross-bridge mechanochemistry using exceedingly rapid changes in the length of activated muscle fibers. The underlying concept of this so-called quick release experiment is that a very rapid release of the tension borne by cross-bridges would drive their dissociation from the thin filament, or at least a change in their conformation. Any transient response in the tension of the contracting fiber that would follow from that quick release would therefore represent the temporal dynamics of the mechanochemistry of the cross-bridge (**Figure 2**). Moreover, very quick releases would allow one to probe the most rapid events associated with the cross-bridge cycle. Thus, the dynamics of force generation are characterized with several phases of tension recovery (T1, T2, T3, and T4 phases).

Rapid release and rapid stretch experiments continue today, contributing significantly to the methods of experiments carried out on muscle fibers. These approaches have been complemented by a host of other experimental efforts, including force measurements in isometric and isotonic conditions for muscle fibers that are either intact (and electrically activated) or chemically skinned

and activated by controlling the concentrations of calcium and ATP. In addition, the advent of powerful tools such as time-resolved X-ray diffractometry and optical tweezers for manipulating or measuring processes at the nanometer scale has yielded significant insight into the dynamics of force production of single molecules (175).

The current paradigm for muscle contraction built upon the sliding filament hypothesis and more than 50 years of research since its development has culminated in a generally accepted view of muscle contraction (for reviews, see 46, 175). Briefly, the notion held by the field today is that cross-bridges use chemical energy derived from ATP hydrolysis to drive axial sliding motion between the thick and thin filaments. The sliding of the filaments is regulated by electrical, chemical, and structural components. Electrical activation of the cell leads to depolarization in the T-tubules, the opening of calcium channels, and the subsequent calcium-induced calcium release from the sarcoplasmic reticulum into the myofibril (in an elegant process termed E-C coupling). While the muscle is relaxed, the troponin–tropomyosin complex blocks myosin-binding sites on the thin filament. However, when calcium enters the system, it binds with the troponin–tropomyosin complex, inducing a conformational change that reveals the binding sites and allows cross-bridges to form. Upon binding, cross-bridges release mechanical strain energy derived from ATP hydrolysis and generate force, which drives muscle contraction.

In the sections that follow, we review both current and past research efforts with an eye toward highlighting the multiscale features of muscle and the multidisciplinary approach that investigators have used. Beginning with molecular levels of organization, and culminating in cellular and tissue scales, we summarize selected experimental and theoretical approaches that have shaped our understanding of muscle function.

## 2. THE MOLECULAR DRIVER OF FILAMENT SLIDING: SINGLE MYOSIN STRUCTURE, KINETICS, AND MECHANICS

The linchpin theory of cross-bridges acting as independent force generators and the model developed by Huxley & Simmons (72) in 1971 were unique among the other theories of muscle contraction emerging at the time in that they accounted for the following characteristics of muscle contraction (69): (*a*) Tension depends on the extent of filament overlap; (*b*) the maximum speed of shortening is independent of filament overlap; (*c*) the energetic cost of contraction per unit length decreases with increased speed of shortening, implying cyclic interactions, as were proposed by Needham (129) even before the sliding filament theory was developed; and finally (*d*) muscle contracts even when the distance between the filaments is varied, suggesting that contraction does not strictly depend on the spacing of the myofilament lattice. The sliding filament theory also emerged at the same time as the discovery of the collective behavior of myosin motors in other systems, lending credence to the idea that myosin molecular motors work in concert to produce muscle contraction. In this section, we describe the structure and mechanics of individual force-generating myosin motors and their regulation within the contractile lattice.

### 2.1. Single-Myosin Protein Structure and the ATPase Cycle

Each myosin within the thick filament is a hexameric protein comprised of two myosin heavy chains and four myosin light chains (for a review, see 46). The C-terminal end of myosin is rod shaped, and a dimerization of the two heavy chains is structured as an α-helical coil, known as the S2 fragment. The S2 segments of approximately 300 myosins bundle, forming the thick filament backbone. The two heavy chains of each myosin separate and branch, creating two independent

globular regions, known as S1 heads. Each S1 head contains a nucleotide-binding pocket where ATP is hydrolyzed to provide the energy for contraction. S1 heads also contain a region that interacts with actin during cross-bridge cycling. Each myosin heavy chain associates with two light chains: the essential light chain that is required for myosin function and a regulatory light chain that modulates the kinetics of cross-bridge cycling.

The cyclic myosin–actin interactions powering contraction are fueled by ATP in a process known as the chemomechanical cross-bridge cycle (20, 46) (**Figure 2**). In relaxed muscle, most myosin heads are not associated with actin, but instead are bound with ADP and inorganic phosphate (Pi) from the preceding ATP hydrolysis. In this conformation, the actin-binding surface of myosin has polar and charged residues that can associate with actin when tropomyosin is not blocking the binding sites on actin. Myosin initially binds to actin via electrostatic interactions (weak binding), positioning the S1 head so that strong, hydrophobic interactions develop. Force and strain develop when myosin isomerizes in a ratchet-like motion, releasing Pi and generating the powerstroke. Once ADP is released, there is a brief moment when myosin is in rigor. At that moment, ATP rapidly binds in the nucleotide-binding pocket, and this myosin–ATP state reduces the affinity of myosin for actin, allowing cross-bridge detachment and a recovery stroke of the S1 head. ATP hydrolysis is thought to occur mainly in this detached state of myosin, both in resting and contracting muscle, which reprimes myosin for subsequent cycles of cross-bridge formation.

## 2.2. Mechanics and Dynamics of Myosin Motors During Contraction

From their early work on tension transients following a quick release of activated muscle fibers, Huxley & Simmons (72) deduced that each motor molecule, when attached to actin, undergoes a small number of successive movements, each more energetically favorable than the last, thus providing a conceptual basis for the cross-bridge cycle (72). Combining the quick-release protocol with time-resolved X-ray diffraction analyses in single intact skeletal muscle fibers, Piazzesi et al. (139) provided some of the first in situ measurements of the average axial motion of the center of mass of myosin motors relative to the thick filament. With approximately 1-Å resolution, they found that the motion of myosin heads is best explained by working stroke models rather than by rapid attachment and detachment models of actomyosin, supporting the tilting lever arm hypothesis (139). This was later confirmed by Hugh Huxley and colleagues (78), who showed that the center of mass of myosin heads moves with, on average, a tilt of approximately 60° during the working stroke.

Understanding the forces that drive filament sliding and sarcomere shortening during contraction required a closer look at myosin motor mechanics and dynamics in intact muscle. Vincenzo Lombardi and Gabriella Piazzesi, both of whom trained under Andrew Huxley, provided novel insights into the in situ motions and mechanics of the myosin motor during muscle contraction. For example, in isometric contractions, there is an elastic distortion of the myosin motors of approximately 2–2.7 nm (contributing 40–50% of the sarcomere compliance), allowing for the development of force during contraction against high loads (27). Furthermore, by monitoring the axial motion of the myosin heads during the force response to a sudden decrease in fiber length, Piazzesi and colleagues (138) demonstrated that the force–velocity relationship in skeletal muscle is determined by a modulation of the number of myosin motors (each with constant force and stroke size) rather than the force-generating capacity of individual motors. In fact, it was later estimated by the same group that as few as 1–4 myosin motors per half-thick filament could provide maximum (unloaded) shortening in muscle (39) with a working stroke size of approximately 7 nm (137). Huxley's original model attributed this relationship to a lower force exerted per myosin

motor (68). Similarly, Caremani et al. (16) recently demonstrated that the size and speed of the working stroke of cardiac myosin ranges from 3 to 8 nm and 1,000 to 6,000 $s^{-1}$ depending on the load against which the muscle is contracting. Additionally, the force per myosin motor during an isometric twitch in cardiac muscle is similar to that of fast myosin in skeletal muscle [approximately 6 pN (9, 95)] but has a stiffness that is two- to threefold smaller than skeletal muscle myosin (140).

### 2.3. Structure–Function Relationships of Myosin from Pathological and Therapeutic Perspectives

Our understanding of myosin structure and function in normal, healthy muscle paved the way for studies examining the functional consequences of altered myosin structure in disease. For example, a study focused on R403Q myosin mutation associated with hypertrophic cardiomyopathy (193) showed that a heart disease associated with ventricular hypertrophy and diastolic dysfunction can have a single-molecule basis. The R403Q mutant myosin isolated from murine hearts has significantly increased actin-activated ATPase rates and higher average (ensemble) force production compared to normal (wild-type) myosin but no differences in single-myosin force production (193). More recent studies using recombinant human cardiac myosin found that R403Q mutant myosin has a reduced affinity for actin and reduced ATPase rates and produces less intrinsic force compared to wild-type myosin (127). The range of functional properties for the R403Q myosin mutation has sparked debate about whether organ-level hypercontractility scales down to the single-protein level and, more generally, about the mechanisms by which mutated proteins drive organ-level remodeling and dysfunction.

With advances in tools for investigating structural dynamics of myosin (e.g., small-angle X-ray diffraction, X-ray crystallography, time-resolved fluorescence microscopy, computational modeling), possible structural bases for cardiomyopathies linked to mutations in cardiac myosin have begun to emerge (176). A commonality among many mutations in myosin associated with hypertrophic cardiomyopathy appears to be the inability of myosin motors to sufficiently turn off or become unavailable for ATPase activity. This overactivity is likely due to the mutation-induced, allosteric restructuring of myosin that disrupts intra- and intermolecular interactions that would otherwise stabilize the resting conformation. Motors that are unable to rest during diastole likely have an increased probability of forming force-generating cross-bridges during systole, therefore contributing to pathological hypercontractility (128, 177, 204). The opposite case may also be true—mutations in myosin found in patients with dilated cardiomyopathy (a disease associated with hypocontractility) have been found to inhibit the ability of myosin to fully activate during systole (204).

The altered myosin motor structure caused by mutations associated with cardiac dysfunction raises the question of whether myosin structure can be targeted for therapeutic intervention. Some myosin-targeted small molecules [e.g., Omecamtiv Mecarbil (201) and 2-deoxy-ATP (115, 143)] have been shown to alter myosin structure, providing beneficial functional effects.

## 3. THE FILAMENTS THAT SLIDE, PULL, AND STRETCH: MYOFILAMENT STRUCTURE, MECHANICS, AND REGULATION

All of the dynamics discussed above play out in a lattice of compliant myofilaments. Thus, the forces generated by single molecules collectively interact at a higher level of organization. In this section, we review the mechanical, geometric, and regulatory features of the key filaments that comprise the lattice.

### 3.1. Thin Filament Structure, Mechanics, and Regulation of Contraction

Thin filaments are approximately 1.1 μm long in vertebrate striated muscle and are composed of a double-helical coil of filamentous (F)-actin, laced along its length with tropomyosin strands (188). Each double-stranded tropomyosin covers seven globular (G)-actins along each helical strand of F-actin. Troponin complexes contain a calcium-binding (TnC), an inhibitory (TnI), and a tropomyosin-linking (TnT) subunit on each strand of the thin filament, such that there is a ratio of seven actins to one tropomyosin and one troponin complex (7:1:1), often called a structural regulatory unit. In the absence of calcium, inhibition of contraction occurs because tropomyosin strands lie in a position blocking the myosin binding sites on each G-actin of the thin filament, a position that is stabilized by TnI interaction with two actins (one on each F-actin strand).

Following a cellular action potential, release of calcium from the sarcoplasmic reticulum leads to thin filament activation. Calcium binds to the N-terminal lobe of TnC, exposing hydrophobic residues and increasing the affinity of the N-terminal lobe of TnC for TnI, which reduces the affinity of TnI for actin (22). The reduced affinity of TnI for actin increases tropomyosin mobility on thin filaments, exposing myosin-binding sites on actin (116). Myosin binding to actin results in further displacement of tropomyosin and prevents tropomyosin from moving back to a blocking position (203). When calcium dissociates from troponin, myosin motors detach from actin progressively, allowing tropomyosin to move back to an inhibitory position on the thin filament and sarcomere relaxation to ensue.

To see how regulatory events in thin filaments influence larger-scale function, it is helpful to examine the differences between cardiac and skeletal thin filament activation. In mammals, fast skeletal muscle TnC has two N-terminal calcium-binding trigger loops (62, 66) that ensure rapid thin filament activation and exposure of more than the 11 actin monomers of the structural regulatory unit, i.e., binding sites are thought to be exposed in neighboring regulatory units as well (156). This has been suggested to be a mechanism of cooperative activation in fast skeletal muscle, and computational models that account for cooperativity in thin filament activation support this notion (14). In contrast, cardiac TnC has only a single calcium-binding loop, and calcium bound in this loop is insufficient to expose hydrophobic residues of TnI (170), reducing the ability of calcium binding alone to completely activate thin filaments (196). Cardiomyocytes therefore rely on additional mechanisms of thin filament activation, such as cooperative activation between neighboring regulatory units along the thin filament (147) and cross-bridge binding (14). Studies have shown that myosin binding to actin increases TnI affinity for TnC, although the size of the functional regulatory unit is thought to be seven actin monomers or fewer (43). Thus, a combination of cross-bridge binding and calcium binding to neighboring troponins may be required for full activation of a regulatory unit in cardiac muscle. Furthermore, while skeletal muscle can modulate calcium-activated force based on firing frequency and/or recruitment of motor neurons innervating each cell, cardiac muscle activation is restricted to individual, cellular-level mechanisms.

Because cardiac thin filaments are less sensitive to calcium than are skeletal muscle thin filaments, modulation of myosin motors in cardiac muscle can also augment activation kinetics (and force) (90). Moreover, as thin filament activation in cardiac muscle depends on myosin, cross-bridge detachment when calcium dissociates from troponin can facilitate a more rapid deactivation of the thin filament and return of the muscle to rest (132). This is one mechanism of rapid deactivation that allows for rapid relaxation as heart rate increases via adrenergic modulation during stress. Another mechanism that provides an increased rate of relaxation in cardiac muscle with adrenergic stimulation is phosphorylation of cardiac TnI (86), a mechanism that is not available to skeletal muscle. This is accomplished with a cardiac-specific N-terminal extension on TnI (174) that contains phosphorylation sites. When these sites are phosphorylated, they interact with

another region of TnI, the inhibitory peptide, to destabilize the interaction between TnI and TnC (19, 197), precipitating calcium release from TnC and deactivation of troponin and the thin filament.

## 3.2. Thick Filament Structure and Composition

The thick filament of mammalian striated muscle is approximately 1.8 μm long and consists mainly of myosin arranged as a helical, bipolar filament. The α-helical coiled coils of the myosin tails form the backbone of the thick filament, and the myosin heads (two per molecule) extend outward radially from the surface of the backbone (202). The central portion of the thick filament (the M-line) is bare of myosin motors and contains unique titin protein domains and other proteins, such as myomesins, that physically link thick filaments together at the M-line (40, 41). Myosin motors are arranged on the thick filament as crowns of three heads, and each head within the crown is separated azimuthally from the others by 120° (102, 149, 178). Subsequent crowns along the axis of the thick filament are separated by approximately 14.3 nm (**Figure 3**) and rotated azimuthally by 40° such that the myosin head helical periodicity along the thick filament is approximately 43 nm (149, 178).

These structural details are supported by imaging data from high-intensity X-ray light. The bipolar arrangement of myosin heads along the thick filament axis produces unique X-ray diffraction patterns that, with today's advances in photon detectors, enable high spatiotemporal-resolution measurements of the position and dynamics of motors during contraction. For example, one feature of the pattern (the meridional reflection or M3) corresponds to the axial distribution

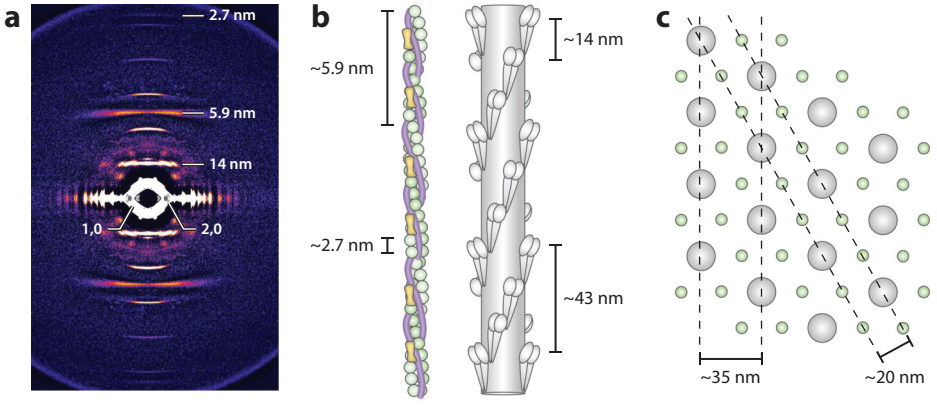


**Figure 3**

The geometry of the myofilament lattice can be revealed by X-ray diffraction. (*a*) An X-ray diffraction pattern of the synchronous flight muscle from *Manduca sexta* taken at the Advanced Photon Source at the Argonne Laboratory. The layer lines correspond to the axial and radial reflections of the pseudocrystalline structure of the sarcomeres. The vertical axis of reflections corresponds to axially periodic structures along the filaments, while the horizontal axis corresponds to reflections caused by the filament lattice in the radial direction. (*b*) An axial view of resting thin and thick filaments. Actin monomers are approximately 2.7 nm apart along the double-stranded filament, which has a helical periodicity of approximately 5.9 nm. Myosin motors are arranged axially as crowns of three motors every approximately 14 nm. With an azimuthal rotation of approximately 40°, the helical periodicity of the myosin crowns repeats every three crowns, or approximately 43 nm. (*c*) The arrangement of the myofilament lattice produces two planes of symmetry: one that is produced by neighboring thick filaments separated by approximately 35 nm and a second that is produced by both thick and thin filaments separated by approximately 20 nm.

of myosin crowns along the thick filament (**Figure 3**). If the spacing of the crowns was perfectly uniform along the thick filament, then a single M3 intensity distribution would occur. However, mirrored myosin structures on each half of the thick filament produce intensity distributions at higher spatial frequencies (in reciprocal space) compared to the distribution from the crown repeats, and with enough intensity, these higher-order interference fringes can cause a splitting of the M3 peak into two narrower peaks (58; for a review of the M3 split, see 149). Recent analyses of the split M3 reflection can inform our understanding of the in situ axial motions of myosin heads during contraction (78, 96, 139, 152, 153) and quantify the fraction of myosin motors in resting, active, or force-generating states (151).

Recent studies have focused on myosin-binding protein-C (MyBP-C), another important thick filament–associated protein that localizes to the central third of the half-A-band (144), to determine its role in regulating contraction. In mammals, MyBP-C is expressed in three isoforms, slow skeletal, fast skeletal, and cardiac, and the functional role varies among the isoforms (93), as is discussed briefly in Section 3.3. MyBP-C consists of multiple serially linked immunoglobulin and fibronectin domains and a unique linker domain that serves as a phosphorylation site. As its name suggests, MyBP-C binds to myosin and the thick filament backbone via its C-terminal domains, while the first four N-terminal domains of MyBP-C [consisting primarily of immunoglobulin (Ig) domains and phosphorylation sites] can interact with the thin filament (146, 148, 165) and myosin S2 on the thick filament (52).

## 3.3. Thick Filament–Based Regulation of Contraction

Recent evidence points to the thick filament as an additional component of the contractile regulatory system in striated muscle. This regulatory mechanism relies, in part, on feed-forward mechanosensation in the myosin filament: Stress in the thick filament backbone (caused by force-generating motors or passive sarcomere stretch) is thought to disrupt what are likely electrostatic interactions that stabilize resting myosin heads in the interacting head motif (202), thereby recruiting motors for force generation in a stress-dependent manner. Motors stabilized in this conformation [referred to as the OFF state (94) or the super-relaxed state (117)] are folded back onto the thick filament backbone with their heads pointing toward the M-line of the sarcomere (150), making ATP hydrolysis unfavorable. Support for this mechanism was recently provided by time-resolved X-ray diffraction measurements of thick filament structure coupled with measurements of sarcomere-level mechanics. During isometric tetanus in skeletal muscle fibers, stress in the thick filament backbone develops after calcium-mediated thin filament activation and progressively switches myosin motors ON during tetanus (94). Moreover, in the absence of calcium, passive stretch-induced thick filament strain releases resting motors, likely through mechanisms similar to those facilitating contraction (38).

The thick filament mechanosensing hypothesis has also been tested in mammalian cardiac muscle (15, 108, 136, 151). During a cardiac twitch, myosin motors are released from their resting state in proportion to systolic force (151). Thus, as venous return and metabolic demands vary beat to beat, cross-bridge recruitment is proportionately tuned to meet contractile demands, thereby optimizing the energetic efficiency of systole–diastole cycles. Moreover, the axial distribution of myosin recruitment along the thick filament backbone may be affected by MyBP-C. As force develops during a cardiac twitch, motors in the c-zone of the A-band are recruited first and support the majority of the force during the twitch (10). The resting structure of the thick filament may be a promising therapeutic target to treat systolic heart failure (4, 143).

The function and regulatory role of MyBP-C in the sarcomere are areas of active investigation (10, 57, 118, 119, 125). MyBP-C may stabilize the resting conformation of myosin motors and may

therefore regulate their release upon activation (119). Ablation of MyBP-C increases cross-bridge binding and cycling rates, likely by removing the physical constraints of MyBP-C on the myosin motors (181). This mechanism has also been explored as a potential treatment for diminished cardiac contractile function in dilated cardiomyopathy (92). Additionally, although MyBP-C is mainly associated with the thick filament, recent evidence has emerged that it can also interact with actin, forming interfilament cross-links that may facilitate thin filament activation (56, 126, 158). Similarly, the protein myomesin bridges thick filaments together at the M-line, which likely regulates both axial and radial myofilament dynamics during contraction (191).

### 3.4. Titin Structure and Mechanics

The early two-filament model of the sarcomere proposed by Huxley and colleagues could not explain all of the mechanical properties of resting muscle. An additional elastic element was needed to account for passive tension and stiffness in the sarcomere (independent of actin–myosin interactions), but such an elastic element was not discovered until many years after the initial Huxley models. Passive elements could, for example, include contributions from the extracellular matrix, the Z-disks, and various protein constituents, including the giant filamentous protein titin, which spans the length of the entire half-sarcomere in muscle. It is the largest known protein (3–4 MDa) and is composed of many unique, serially linked domains that have specialized tasks in the sarcomere. Historically, titin was believed to be mainly a structural protein that connected the thick filament to the Z-disc and was initially aptly named connectin by Maruyama and colleagues (111, 112). Titin has been found to be a highly dynamic and complex protein, involved in multiple mechanical and biochemical aspects of muscle function. As many features of titin have been comprehensively reviewed elsewhere (35, 49, 50, 97, 99), we explore how recent information about the mechanical properties of titin has shaped our interpretation of the sliding filament theory in resting and contracting muscle.

While the structure and length of the I-band region of titin varies among muscle types and titin isoforms (50), it generally consists of dozens of serially linked Ig domains that flank a distinct region rich in proline (P), glutamate (E), valine (V), and lysine (K), termed the PEVK region, and a unique amino acid sequence that varies among isoforms and muscle types (the skeletal N2A region and the cardiac N2B or N2BA region). The A-band region of titin is less understood than the I-band region. It consists of Ig and fibronectin super-repeats that strongly interact with myosin and MyBP-C (99), and it is likely much stiffer than the I-band region (29). Each super-repeat is approximately 43 nm in length, which coincides with the helical repeat distance of myosin crowns along the thick filament (36). It has therefore been hypothesized that the A-band region of titin facilitates myosin filament formation and structure (189). Tonino et al. (189) recently showed that deleting two super-repeats in the A-band of murine cardiac and skeletal muscle causes a significant reduction in the length of the myosin filament. This change in thick filament length alters the sarcomere length dependence of force and reduces contractility in both cardiac and skeletal muscle (189).

The mechanical properties of the I-band region of titin contribute significantly to the total passive elasticity of muscle (48, 51, 80). Titin expressed in mammalian skeletal muscle is generally longer and therefore effectively more compliant than cardiac muscle titin. Using fluorescent probes positioned proximally and distally to the PEVK segment, Linke and colleagues (100, 101) showed that Ig domains extend first, and that the length of the PEVK segment is preserved until much longer sarcomere lengths. Moreover, studies on whole titin molecules (85, 110) and isolated titin fragments (109, 157) have shown that individual Ig domains dynamically unfold and refold under load, and that nearly all Ig domains are likely to be unfolded in random order at

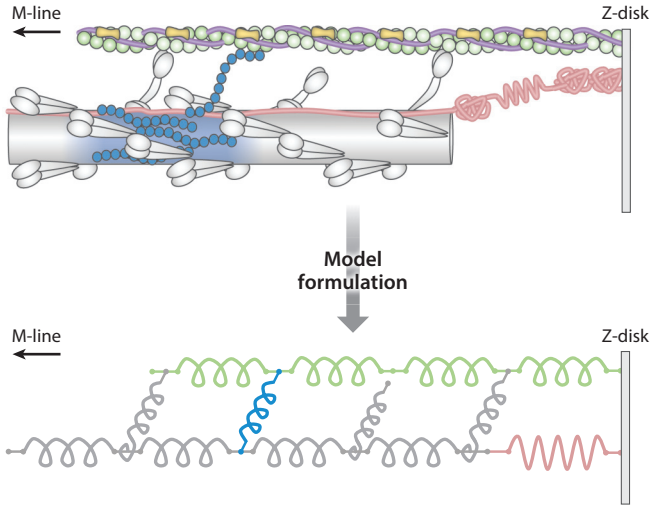


**Figure 4**

An example of the half-sarcomere represented as a system of springs in computational and mathematical models. Computational and mathematical models of muscle function often rely on dissecting complex sarcomere–protein interactions into a system of Hookean springs. Models such as these provide approximations of mechanics, energetics, and kinetics of contraction and relaxation that can accurately recapitulate experimental observation and/or generate experimentally testable hypotheses. Myosin cross-bridges can be modeled as two-spring systems (*gray*) consisting of a linear spring plus a torsional spring at the thick filament backbone (198), and MyBP-C (*blue*) can be modeled as a spring in parallel with cross-bridges (37). Titin can also be modeled as an additional spring in the I-band (*pink*), in parallel with the thin filaments and the array of cross-bridges (141, 142).

approximately 10 pN (8, 159). Mártonfalvi et al. (110) suggest that exposure of ligand-binding sites on titin may provide a mechanoregulated signaling motif to the I-band.

The load-dependent structural dynamics of the Ig domains in the I-band region of titin (159), together with the spring-like characteristics of the PEVK segment (100), provide the sarcomere with a length-dependent spring. A recent study used a mechanical model of the half-sarcomere (134) (**Figure 4**) to provide an in situ quantitative description of the elasticity of the I-band region of titin during tetanic contraction (141). The stiffness of titin during contraction at long sarcomere lengths is approximately 6 pN/nm, a value that is approximately 100 times larger than the static stiffness responsible for the passive force–length relationship in resting muscle over the same range of sarcomere lengths (141). Similarly, changes in titin stiffness (e.g., due to phosphorylation or disease-causing mutations) may affect the force-generating capacity of myosin motors (142).

The apparent stiffness of the I-band region of titin in vivo depends on factors such as phosphorylation (54, 61, 89), interactions with actin (100, 130), calcium-dependent stiffness upon muscle activation (28), and isoform switches during development or disease progression (49). Ongoing research efforts aim to elucidate the relationship between altered titin stiffness and muscle function, especially in disease contexts.

## 3.5. Titin-Based Regulation of Contraction

The regulatory and structural roles of titin in contraction remain an active area of research. The I-band region of titin physically links the thick filament to the Z-disk and likely facilitates

mechanical force transmission between the Z-disk and the myosin filament. Accordingly, during muscle contraction, titin may play a role in force equilibration, balancing axial forces within the sarcomere (142) or between serially linked sarcomeres during contraction (111, 195).

Titin may also be involved in activating the other myofilaments in the sarcomere by transmitting forces between them during passive stretch. Recent work by Fusi et al. (38) suggests that titin may facilitate thick filament activation in skeletal muscle by imposing stretch-induced stress on the thick filament backbone, disrupting the resting conformation of myosin motors. Moreover, the shorter sarcomere lengths at which cardiac muscle operates (compared to skeletal muscle) suggest that the shorter titin molecule in cardiac muscle may be tuned to provide mechanical functions similar to those of cardiac muscle (107, 108). The I-band region of titin in mammalian cardiac muscle was recently implicated in length-dependent activation of both thick and thin filaments, likely through a cooperative, strain-dependent mechanism upon stretch (2).

The A-band region of titin also plays a role in biochemical signaling. Indeed, titin binds to more than 25 other proteins (99). Many titin-associated ligands, such as calmodulin, filamin C, and obscurin, interact with the M-band region of titin (99). Furthermore, the M-band region of titin interacts with muscle-specific RING-finger proteins-1/2 (MURF1/2), which bind to microtubules and help maintain their stability (49, 99). Lastly, myomesin interacts with the M-band region of titin, which provides links between thick filaments (98).

Notably, the A-band region is also associated with cardiomyopathy-causing mutations. Approximately 25% of patients with end-stage dilated cardiomyopathy have titin-associated truncating mutations (60), many of which are located in the A-band region of titin. In cardiomyocytes lacking full-length titin, myofibrils are more susceptible to damage during mechanical loading compared to cardiomyocytes with full-length titin (167). However, depending on the location of the truncation-causing mutation, a recently discovered shorter isoform of titin [called Cronos titin (206, 207)] can facilitate myofibrillar organization in the absence of full-length titin, which can partially preserve cardiac contractility in human cardiac myocytes (206).

## 4. A MICROSCALE MACHINE OF SLIDING FILAMENTS: SARCOMERE STRUCTURE, ORGANIZATION, MECHANICS, AND DYNAMICS

Just as individual motor proteins generate forces and interact within a lattice of compliant, regulated myofilaments, the scaffolding of filaments within the whole sarcomere connects function across scales. Among the earliest experimental results connecting these spatial scales was the classic length–tension relationship established by Gordon et al. (47). The discovery of this relationship was instrumental in supporting the sliding filament hypothesis and theory of independent force generators and highlighted the notion that muscle force depends on its geometric state (32). In this section, we explore recent experimental and theoretical advances that have revealed additional geometric and dynamic features of force generation at the sarcomere scale. These advances have resulted from emerging techniques for time-resolved data and computational methods that were not feasible at the onset of the sliding filament hypothesis.

### 4.1. Structure and Organization of the Lattice

A host of imaging technologies have been brought to bear in our understanding of the structure and organization of the myofilament lattice and sarcomeres of striated muscle. These include EM, X-ray diffraction, laser diffraction, and fluorescence confocal microscopy. EM was among the earliest imaging technologies used to reveal sarcomere structure (55). Although EM directly reveals the layout of electron-dense structures with extremely high spatial resolution [recent

microscopes approach sub-Angstrom resolution (161)], the tissue fixation that it requires can alter the sizes, spacing, and organization of subcellular structures. In contrast, X-ray diffraction patterns of muscle can reveal the myofilament lattice geometry without the need for fixation (or any modification of the muscle tissue) (178). Indeed, muscle X-ray diffraction can be done on intact whole animals and muscles (42, 105). Early X-ray diffraction experiments beginning in the 1940s (7) required long exposure times, precluding detailed measurements of the temporal dynamics of active muscle until the 1960s (30, 75). With the advent of powerful synchrotron radiation and high-speed digital detectors in the 1980s, time-resolved experiments exceeding 100 Hz became possible (76, 82), enabling measurements of axial and radial structural changes of the sarcomere in active muscle.

In mammalian skeletal muscle, the interdigitating myofilaments in the overlap region of the sarcomere are arranged in a three-dimensional lattice with a double-hexagonal symmetry that enables cross-bridges from multiple thick filaments to interact with a single actin filament (**Figure 3**). In the I-band region, the thin filaments form a rectangular lattice as they insert into the Z-disk (180). However, the myofilament packing ratio and lattice geometry vary considerably across different animal taxa (67), suggesting that structural adaptations in the lattice enable functional specialization (168). For example, packing ratios of thick to thin filaments can vary from 6:1 in cockroach leg muscles (53) to 5:1 in *Lethocerus* (190) and 12:1 in the common garden snail (162). Interestingly, variation in features like packing ratio not only impacts the number of available binding sites, but also may affect other aspects of structural mechanics, such as electrostatics, filament lattice spacing, and cross-bridge kinetics. This is an area that is ripe for future research.

Extending from the theory of independent force generators, another theory is that muscles with many short sarcomeres connected in series will be well adapted to rapid contraction, while muscles with longer sarcomeres (and myofilaments) are better suited to slower, high-force contractions (53, 71). This theoretical hypothesis is born out in structure–function relationships seen across taxa (131) and even across muscle groups within a single organism, where both the packing ratios of thick to thin filaments and the filament lengths are correlated with either large forces or rapid contractions (168).

In the 1970s, an alternative hypothesis to the theory of independent force generators suggested that electrostatic forces drove muscle contraction (31, 69, 124, 166). However, the theory that filament sliding is due to independent force generators took precedence over that alternative hypotheses (70), diminishing interest in electrostatic interactions. We know today, however, that such interactions help stabilize the lattice (160, 171). The repulsive forces between negatively charged filaments and constricting forces (likely arising from elastic structural components such as the Z-disks; M-line proteins like myomesins; and proteins like titin and MyBP-C, which are interwoven in the myofilament lattice) yield a stable equilibrium (123). Independent of steric interactions with cross-bridges, the thin filaments are more subject to collapse at low pH than are the thick filaments (113), although at normal pH the lattice does not collapse, indicating the importance of mechanical forces. While either electrostatic forces alone (122) or mechanical forces alone (171) can roughly account for lattice spacing, the data are best fit by models that take both electrostatic and mechanical forces into account (171).

In addition to stabilizing the lattice, the charges of lattice proteins also attract polar water molecules, resulting in a layer around filaments. In total, approximately 30% of the lattice volume is osmotically inactive, with approximately 20–25% taken up by protein (121). The remaining fluid in the lattice is free to flow and could mediate substrate transport, as is discussed further in section 4.2.

## 4.2. Radial Sarcomere Dynamics and Interfilament Regulatory Mechanisms

In addition to the packing ratio of thick to thin filaments, the radial spacing of filaments can also vary between species and temporally during contraction. By its name, the sliding filament hypothesis gives the impression that the radial spacing of the myofilaments does not vary during contraction. However, as muscle contracts and relaxes, the spacing between myofilaments in the lattice changes, which has important implications for myosin motor binding kinetics, fluid flows, and radial elastic energy storage. Decreased lattice spacing can bring myosin molecular motors closer to the thin filament, thus increasing the probability of cross-bridge binding (1, 17). Additionally, changes in lattice spacing alter the strain in bound cross-bridges and the direction of the forces that they apply (163). Spatially explicit modeling of the system corroborates experiments, highlighting that lattice spacing is an important regulator of axial muscle force (184, 186, 198, 200). Given its importance for muscle function, it is important to understand what the rules are that govern lattice spacing.

Early X-ray diffraction experiments showed that resting muscles maintained a constant volume, with the lattice dilating as sarcomeres shortened and constricting upon sarcomere lengthening (30, 160). The lattice also maintains a constant volume during length changes in resting fibers of the crayfish leg, where 12 thin filaments surround each thick filament (5). However, because cross-bridges produce axial and radial forces, the isovolumetric hypothesis cannot be fully tested in resting fibers. In the 1990s, time-resolved X-ray diffraction patterns of active muscles revealed that cross-bridges exert radial forces that compress the filament lattice, demonstrating that the lattice is not isovolumetric (17, 18). Furthermore, in one of the first in vivo X-ray diffraction experiments, the lattice spacing of *Drosophila*'s cyclically contracting flight muscle was shown to be constant during natural function (81). In contrast, X-ray diffraction patterns from the cyclically contracting flight muscle of *Manduca sexta* revealed that the lattice dilates and compresses, but there is considerable variation among individual animals in both the magnitude and temporal patterns of lattice kinematics (105). Additionally, the dynamics of lattice spacing are also correlated with naturally occurring temperature gradients within the thorax (42). Moreover, differences in lattice spacing as small as 1 nm have been correlated with the distinct functional roles (e.g., mechanical work) played by adjacent cockroach leg muscles that are otherwise identical (42, 192). Thus, feedback between active cross-bridges and the radial lattice spacing can control the temporal dynamics of work and force in contracting muscle.

The dense packing of filaments has been shown to slow the diffusion of substrates to their target sites by computational (3, 169) and experimental studies (25, 114, 133), with decreases in lattice spacing decreasing the rate of diffusion (84). Diffusion rates depend on the size of substrates, and the anisotropic structure of the lattice results in more rapid axial diffusion than radial diffusion for some substrate sizes (6, 63). Additionally, diffusion rates may be a driver of organelle positioning within muscle cells. For example, mitochondria are subject to mirrored constraints, including the diffusion of the oxygen necessary for ATP production and the diffusion of ATP into the dense contractile lattice (87). The time constraint imposed by slow diffusion may be especially problematic for cells contracting at high frequencies, where substrate exchange (e.g., calcium, ATP) with organelles sitting exterior to the lattice must occur over rapid timescales.

Diffusion is not the only mechanism that could drive substrate exchange between the lattice and surrounding intracellular environment. Dynamic changes in the volume of the lattice, modulated by cross-bridges, necessitate fluid flow that could have important implications for substrate exchange. Interestingly, using a simplified model of viscous shear stresses for flow between filaments, Andrew Huxley (70) concluded that such stresses are not important. That said, the implications of fluid flow for muscle function are still relatively open areas for muscle research.

The relationship between cross-bridges and lattice spacing is one example of interfilament regulation of the sarcomere that differs from many of the mechanisms that we discuss in Section 3, which focuses on individual filament-associated proteins. Thus, muscle employs multiple regulatory mechanisms, spanning from the scale of single molecules to the dynamic motions of ensembles of myofilaments.

## 4.3. Axial Sarcomere Dynamics and Interfilament Regulatory Mechanisms

The importance of lattice geometry was shown in the classic study by Gordon and colleagues (47), highlighting the dependence of active force on sarcomere length. Three main features emerged from their paper. At long sarcomere length (approximately 3.5 μm), where thick and thin filaments barely overlap, few cross-bridges can contribute to force. Force rises linearly during contraction as sarcomere length decreases to approximately 2.2 μm, where filament overlap allows the maximal number of cross-bridges to form with the thin filaments. This region is called the descending portion of the length–tension relationship (even though it ascends during contraction). From approximately 2.0–2.2 μm, force peaks and remains constant. From approximately 1.3–2.0 μm, force declines linearly as a consequence of steric hindrance among actin filaments, titin, the thick filament, and the Z-disk. This is called the ascending portion of the length–tension relationship. Thus, the power of muscle depends on the sarcomere length at which it is contracting. This length dependence of active force adds to passive tension, which rises exponentially with sarcomere length, which is primarily due to titin (see Section 3.5). It should be noted that, as the lattice expands during contraction, the increased distance between myosin and actin reduces the likelihood of cross-bridge formation, thus also contributing to the decrease in force with decreases in length. Additionally, experiments that involve osmotic compression of the lattice suggest that, at long sarcomere lengths, lattice compression may also inhibit axial force generation by constraining the angle at which cross-bridges can generate axial forces (200). Thus, the force–length relationship may follow from more complex lattice kinematics than were initially suggested in the pioneering work of Gordon et al.

The dependence of force on sarcomere length is also a key determinant of cardiac muscle function. Over a century ago, Otto Frank and Earnest Starling observed in independent studies that the systolic pressure is modulated by diastolic filling, thus providing beat-to-beat regulation of cardiac output. While the subcellular origins of this feature of cardiac muscle, now referred to as the Frank-Starling law of the heart, are still under active investigation (2, 26, 33, 172), the length dependence of tension and calcium sensitivity in cardiac myocytes is generally believed to be an integral component. In particular, cardiac muscle differs from skeletal muscle in that it operates mainly on an ascending limb of the length–tension relationship (16). Consequently, during diastolic filling, when ventricles are stretched, the sarcomere length of resting cardiomyocytes increases, leading to larger forces. A variety of mechanisms may contribute to the sarcomere length dependence of force in cardiac muscle, many of which are under active investigation, such as length-dependent calcium sensitivity of force (26, 88), recruitment of myosin motors (13, 106, 151), and titin strain (2).

In addition to the functional consequences of lattice spacing and length-dependent force generation, filament compliance may play a significant role in regulating muscle function. The idea of compliance as a factor gained attention with a series of papers in 1994 (44, 79, 194) that introduced experimental data pointing to periodicity changes in the thick and thin filaments in relation to the tension that they bore. These papers led to spatially explicit computational models that suggested that, as tension develops in myofilaments, axial strain can realign myosin-binding sites on actin filaments, augmenting cross-bridge recruitment (23). Spatially explicit models with

filament compliance (12, 23, 120) allowed Tanner et al. (185) to explore the influence of the degree of cooperativity between neighboring regulatory units along myofilaments on force output. Additionally, while the study of sarcomere elasticity tends to be dominated by the myofilaments, the functional role of Z-disk compliance is also an active area of research (40, 103).

## 4.4. The Ends of the Sarcomere: Z-Disks and Myotendinous Junctions

The vast majority of muscle research has centered on myofilament structure, regulation, and organization. Far less attention has focused on the Z-disk (Z-line, Z-band), which joins sarcomeres end to end, transmitting forces between sequential sarcomeres. Thin filaments anchor into the Z-disk via α-actinin and nebulin (103). Similarly, titin interacts with actin and α-actinin to mechanically connect thick filaments to the Z-disk (205). Additionally, proteins such as myozenin and γ-filamin (183) and LIM-domain proteins play important roles in the structural integrity of the sarcomere, signaling, and mechanosensing (65, 145). Myriad other Z-disk proteins have been linked to various muscular dystrophies (24) in which crucial structural connections between the sarcomere and the sarcolemmal surface are compromised.

For vertebrate muscle, the thin filament lattice arrangement shifts from hexagonal packing to rectangular packing as it attaches to the Z-disk. The thickness of the Z-disk varies considerably, from approximately 30 nm in fast skeletal muscle fibers to approximately 100 nm in cardiac fibers (104). Interestingly, a recent study shows that the rapidly contracting sonic muscles of the midshipman fish have exceptionally wide Z-disks (approximately 1,200 nm), about the same width as the A-band in these specialized sound-producing muscles (11). The greater thickness in cyclically loaded muscles such as cardiac and sound production muscles raises the interesting question of whether the Z-disk plays a role in elastic energy storage as well as in force transmission.

In a transverse view, the network of α-actinin proteins form one of two possible geometries: a square lattice or a basket weave. Early experiments suggested that the shift in geometry depended on the state of active tension—in relaxed fibers, the proteins form a square lattice, whereas in the active state, the structure resembles a basket weave geometry (45). However, a recent study suggests that tropomyosin movement may influence the shift from square lattice to basket weave independent of the level of the force generation (135). In the end, the roles in elastic energy storage and force transmission for Z-disks and myotendinous junctions (MTJs) remain open areas for future investigations.

Axial force transmission along the train of sarcomeres continues across Z-disks to the MTJ, where the cell is folded extensively as it connects to the extracellular matrix—the degree of folding depends on the fiber type (187). At the MTJ, connections between the lattice and the sarcolemma are mediated by various structure proteins, including dystrophin. Defects in dystrophin proteins compromise the associations of thin filaments with the membrane at the MTJ. Thus, similar to the Z-disk, the MTJ remains an open area for future research in muscle physiology and pathophysiology.

## 4.5. Efficiency Is an Emergent Property of Multiscale Interactions

How efficiently do myosin motors convert chemical energy into mechanical energy? Muscle efficiency was first investigated through the lens of heat (32). Long before the sliding filament hypothesis, Fenn (34) showed that muscle that performs work emits more heat than an isometrically contracting muscle. Huxley (70) noted that any model of muscle contractility must account for the Fenn effect. The modulation of the rates of cross-bridge cycling ultimately provides a mechanistic link between muscle mechanics and chemical kinetics (72, 91), allowing for an explanation of

the Fenn effect. In 1987, Homsher (64) provided an excellent review of the relationship between muscle enthalpy production and actomyosin ATPase.

For a linearly elastic spring, the mechanical energy is the product of the spring stiffness and the square of its distortion. Thus, the energy derived from ATP hydrolysis must be greater than the mechanical work associated with distortion of the cross-bridge (138). However, one challenge in estimating efficiency is decoupling energy-consuming processes in the cell, like ion pumping, from the work performed by cross-bridges themselves. Measurements of efficiency in skinned fibers show that there is considerable diversity across organisms, fast and slow muscle types, and operating conditions (e.g., temperature, load, and velocity) (91, 173). The efficiency of human skeletal muscle is estimated to be approximately 20% (59). Documenting the efficiency of individual myosin motors in the lattice is challenging since, by operating asynchronously, they perform work on negatively strained neighbors (83). To estimate myosin motor efficiency, Sugi et al. (182) recorded the power generated by glycerinated fibers when cross-bridge powerstrokes were synchronized by limiting the amount of ATP in the system to approximately one per myosin motor and using the laser-induced release of caged calcium for activation. Their study showed that the efficiency of individual myosin motors within the filament lattice is, conservatively, 70% (182), which is much greater than previous estimates in vertebrate muscle.

## 5. IDEAS FOR THE FUTURE AND THE MULTISCALE PROBLEM

We are acutely aware of the vast amount of exciting muscle history and research that we have not reviewed in this article, such as the challenging open questions about the evolutionary diversity of muscles and their function, the diverse set of functions that muscles must accomplish, questions about sarcomerogenesis and the underlying developmental processes in which mechanical and genetic regulatory pathways conspire to create nearly paracrystalline structures, and myriad other open questions in the field. We chose instead to set the stage for questions that we have found interesting: those largely related to the challenges for understanding multiscale dynamics of muscle and melding models and experiments.

The muscle in a mouse that weighs only a few grams is not all that different from that in whales weighing many thousands of kilograms: Muscle scales from mice to whales and does so with a structure that is stunningly conserved. However, as discussed in Section 1, the fundamental concepts of muscle contraction (launched with the pair of 1954 papers in *Nature* introducing the sliding filament hypothesis) included evidence of the vast spatial and temporal scales across which mechanisms of muscle function must span. Since then, a common interest has emerged in the field of muscle research: developing a deep mechanistic understanding of the multiscale processes—from atom to organ—that govern muscle function. While such multiscale problems are not unique to muscle, understanding the function of muscle on multiple spatiotemporal scales is central to many areas of active research, from interpreting functional and structural diversity across animal taxa, to engineering new technologies, to developing therapies for muscular pathologies.

To a considerable extent, the extreme spatial organization of muscle with repeated modules lends itself well to multiscale studies. For example, time-resolved X-ray diffraction provides data that reflect geometric changes at the scale of Angstroms and nanometers. When this is coupled with other imaging methods [such as laser diffractometry that can provide micrometer (sarcomere)-scale information], along with force and length measurements at the centimeter scale, simultaneous mechanical and structural data can be acquired across nearly eight orders of magnitude ($10^{-10}$ to $10^{-2}$). Few biological systems lend themselves to such a broad range of immediate spatiotemporal information.

Creating predictive models that span such scales is a challenge. For example, molecular dynamics models now provide deep insight into functional dynamics of single myosin molecules, including interactions with various nucleotides (154, 155). However, such modeling approaches are computationally intensive and cannot be scaled to the millions of interacting molecules that constitute a single sarcomere.

As we describe above, spatially explicit sarcomere-scale models (micrometer) that incorporate lattice geometry (184, 198–200), filament compliance (12, 23, 120), cross-bridge and titin mechanics (142), cooperative binding (184), and thin filament regulation (185) provide insight into the interaction between chemical kinetic and structural features, but they also do not scale well. As with molecular dynamics simulations, the computational demands of these Monte Carlo–based approaches preclude predictions of contractile dynamics at the scale of centimeters (thousands of sarcomeres).

Similarly, more heuristic models of muscle force generation, such as Hill relationships, force–length relationships, and activation dynamics (force–time relationships), allow predictive models of tissue-, limb-, and organ-scale dynamics. However, these approaches give little insight into vastly smaller spatial and temporal scales. A core challenge of understanding muscle function across physical scales is the inherent influence of processes at each scale on processes at other scales. That is, mechanisms from one spatiotemporal scale cannot be easily untangled from mechanisms at adjacent scales. Consequently, models at the molecular level of organization are often quite difficult to apply to larger spatial scales and vice versa. Indeed, the two-way coupling between macroscopic and microscopic scales is a fundamental challenge that we face today. This is particularly true of molecular models driven by Monte Carlo simulations. This challenge of multiscale dynamics will require methods to extract reduced-order behaviors from detailed high-dimensional simulations.

In addition to coupling across spatial and temporal scales, there remain additional open areas of research that reflect coupled processes. For example, the coupling between force and activation is inherent in stretch activation, cooperative binding, and mechanosensing (94) in the lattice. Additionally, recent work points to an interesting, and poorly explored, coupling among volume changes of the lattice, fluid flow, and substrate delivery. Thus, contractions may result in fluid exchange between the lattice and surrounding cell volume, where organelles like the sarcoplasmic reticulum and mitochondria are located. Ultimately, coupling among experimental, theoretical, and computational efforts will enable us to develop models that may be used as tools for understanding disease and for designing novel therapeutics.

## DISCLOSURE STATEMENT

The authors are not aware of any affiliations, memberships, funding, or financial holdings that might be perceived as affecting the objectivity of this review.

## ACKNOWLEDGMENTS

The authors are grateful for scientific discussions with Tom Irving at BioCAT at the Advanced Photon Source of the Argonne National Laboratory. This work was supported by Army Research Office grant W911NF-14-1-0396 and the Joan and Richard Komen Endowed Chair to T.L.D.; a Bioengineering Cardiac Training Grant from the National Institute of Biomedical Imaging and Bioengineering (T32EB1650) and a fellowship from the ARCS Foundation to S.A.M.; National Institute of Arthritis and Musculoskeletal and Skin Diseases grant P30 AR074990, National Heart, Lung and Blood Institute grant HL128368, and European Union grant 777204 to M.R. and T.L.D.; and National Heart, Lung and Blood Institute grant F32 HL152573 to J.D.P.

## LITERATURE CITED


1. Adhikari BB, Regnier M, Rivera AJ, Kreutziger KL, Martyn DA. 2004. Cardiac length dependence of force and force redevelopment kinetics with altered cross-bridge cycling. *Biophys. J.* 87(3):1784–94
2. Ait-Mou Y, Hsu K, Farman GP, Kumar M, Greaser ML, et al. 2016. Titin strain contributes to the Frank-Starling law of the heart by structural rearrangements of both thin- and thick-filament proteins. *PNAS* 113(8):2306–11
3. Aliev MK, Tikhonov AN. 2004. Random walk analysis of restricted metabolite diffusion in skeletal myofibril systems. *Mol. Cell. Biochem.* 256(1/2):257–66
4. Anderson RL, Trivedi DV, Sarkar SS, Henze M, Ma W, et al. 2018. Deciphering the super relaxed state of human β-cardiac myosin and the mode of action of mavacamten from myosin molecules to muscle fibers. *PNAS* 115(35):E8143–52
5. April EW, Brandt PW, Elliott GF. 1971. The myofilament lattice: studies on isolated fibers. *J. Cell Biol.* 51(1):72–82
6. Arrio-Dupont M, Foucault G, Vacher M, Devaux PF, Cribier S. 2000. Translational diffusion of globular proteins in the cytoplasm of cultured muscle cells. *Biophys. J.* 78(2):901–7
7. Astbury WT. 1947. Croonian Lecture—on the structure of biological fibres and the problem of muscle. *Proc. R. Soc. Lond. B* 134(876):303–28
8. Bianco P, Mártonfalvi Z, Naftz K, Koszegi D, Kellermayer M. 2015. Titin domains progressively unfolded by force are homogenously distributed along the molecule. *Biophys. J.* 109(2):340–45
9. Brunello E, Caremani M, Melli L, Linari M, Fernandez-Martinez M, et al. 2014. The contributions of filaments and cross-bridges to sarcomere compliance in skeletal muscle. *J. Physiol.* 592(17):3881–99
10. Brunello E, Fusi L, Ghisleni A, Park-Holohan S-J, Ovejero JG, et al. 2020. Myosin filament-based regulation of the dynamics of contraction in heart muscle. *PNAS* 117(14):8177–86
11. Burgoyne T, Heumann JM, Morris EP, Knupp C, Liu J, et al. 2019. Three-dimensional structure of the basketweave Z-band in midshipman fish sonic muscle. *PNAS* 116(31):15534–39
12. Campbell KS. 2006. Filament compliance effects can explain tension overshoots during force development. *Biophys. J.* 91(11):4102–9
13. Campbell KS, Janssen PML, Campbell SG. 2018. Force-dependent recruitment from the myosin off state contributes to length-dependent activation. *Biophys. J.* 115(3):543–53
14. Campbell SG, Lionetti F V, Campbell KS, McCulloch AD. 2010. Coupling of adjacent tropomyosins enhances cross-bridge-mediated cooperative activation in a Markov model of the cardiac thin filament. *Biophys. J.* 98(10):2254–64
15. Caremani M, Pinzauti F, Powers JD, Governali S, Narayanan T, et al. 2018. Inotropic interventions do not change the resting state of myosin motors during cardiac diastole. *J. Gen. Physiol.* 151(1):53–65
16. Caremani M, Pinzauti F, Reconditi M, Piazzesi G, Stienen GJM, et al. 2016. Size and speed of the working stroke of cardiac myosin in situ. *PNAS* 113(13):3675–80
17. Cecchi G, Bagni M. 1994. Myofilament lattice spacing affects tension in striated muscle. *Physiology* 9(1):3–7
18. Cecchi G, Bagni M, Griffiths P, Ashley C, Maeda Y. 1990. Detection of radial crossbridge force by lattice spacing changes in intact single muscle fibers. *Science* 250(4986):1409–11
19. Cheng Y, Lindert S, Kekenes-Huskey P. 2014. Computational studies of the effect of the S23D/S24D troponin I mutation on cardiac troponin structural dynamics. *Biophys. J.* 107(7):1675–85
20. Cooke R. 1997. Actomyosin interaction in striated muscle. *Physiol. Rev.* 77(3):671–97
21. Cooke R. 2004. The sliding filament model: 1972–2004. *J. Gen. Physiol.* 123(6):643–56
22. da Silva ACR, Reinach FC. 1991. Calcium binding induces conformational changes in muscle regulatory proteins. *Trends Biochem. Sci.* 16:53–57
23. Daniel TL, Trimble AC, Chase PB. 1998. Compliant realignment of binding sites in muscle: transient behavior and mechanical tuning. *Biophys. J.* 74(4):1611–21
24. Davies KE, Nowak KJ. 2006. Molecular mechanisms of muscular dystrophies: old and new players. *Nat. Rev. Mol. Cell Biol.* 7(10):762–73
25. de Graaf RA, van Kranenburg A, Nicolay K. 2000. In vivo 31P-NMR diffusion spectroscopy of ATP and phosphocreatine in rat skeletal muscle. *Biophys. J.* 78(4):1657–64

26. de Tombe P, Mateja R, Tachampa K. 2010. Myofilament length dependent activation. *J. Mol.* 48(5):851–58
27. Dobbie IM, Linari M, Piazzesi G, Reconditi M, Koubassova N, et al. 1998. Elastic bending and active tilting of myosin heads during muscle contraction. *Nature* 396:383–87
28. Dutta S, Tsiros C, Sundar SL, Athar H, Moore J, et al. 2018. Calcium increases titin N2A binding to F-actin and regulated thin filaments. *Sci. Rep.* 8(1):14575
29. Elhamine F, Radke MH, Pfitzer G, Granzier H, Gotthardt M, Stehle R. 2014. Deletion of the titin N2B region accelerates myofibrillar force development but does not alter relaxation kinetics. *J. Cell Sci.* 127(Pt. 17):3666–74
30. Elliot GF, Lowy J, Millman BM. 1965. X-ray diffraction from living striated muscle during contraction. *Nature* 206(4991):1357–58
31. Elliot GF, Rome EM, Spencer M. 1970. A type of contraction hypothesis applicable to all muscles. *Nature* 226(5244):417–20
32. Evans CL, Hill AV. 1914. The relation of length to tension development and heat production on contraction in muscle. *J. Physiol.* 49(1–2):10–16
33. Farman GP, Gore D, Allen E, Schoenfelt K, Irving TC, de Tombe PP. 2011. Myosin head orientation: a structural determinant for the Frank-Starling relationship. *Am. J. Physiol. Heart Circ. Physiol.* 300(6):H2155–60
34. Fenn WO. 1923. A quantitative comparison between the energy liberated and the work performed by the isolated sartorius muscle of the frog. *J. Physiol.* 58(2–3):175–203
35. Fukuda N, Granzier HL, Ishiwata S, Kurihara S. 2008. Physiological functions of the giant elastic protein titin in mammalian striated muscle. *J. Physiol. Sci.* 58(3):151–59
36. Fürst DO, Nave R, Osborn M, Weber K. 1989. Repetitive titin epitopes with a 42 nm spacing coincide in relative position with known A band striations also identified by major myosin-associated proteins: an immunoelectron-microscopical study on myofibrils. *J. Cell Sci.* 94:119–26
37. Fusi L, Brunello E, Reconditi M, Piazzesi G, Lombardi V. 2014. The non-linear elasticity of the muscle sarcomere and the compliance of myosin motors. *J. Physiol.* 592(5):1109–18
38. Fusi L, Brunello E, Yan Z, Irving M. 2016. Thick filament mechano-sensing is a calcium-independent regulatory mechanism in skeletal muscle. *Nat. Commun.* 7:13281
39. Fusi L, Percario V, Brunello E, Caremani M, Bianco P, et al. 2017. Minimum number of myosin motors accounting for shortening velocity under zero load in skeletal muscle. *J. Physiol.* 595(4):1127–42
40. Gautel M. 2011. The sarcomeric cytoskeleton: Who picks up the strain? *Curr. Opin. Cell Biol.* 23(1):39–46
41. Gautel M, Djinović-Carugo K. 2016. The sarcomeric cytoskeleton: from molecules to motion. *J. Exp. Biol.* 219(2):135–45
42. George N, Irving T, Williams C, Daniel T. 2013. The cross-bridge spring: Can cool muscles store elastic energy? *Science* 340(6137):1217–20
43. Gillis TE, Martyn DA, Rivera AJ, Regnier M. 2007. Investigation of thin filament near-neighbour regulatory unit interactions during force development in skinned cardiac and skeletal muscle. *J. Physiol.* 580(2):561–76
44. Goldman YE, Huxley AF. 1994. Actin compliance: Are you pulling my chain? *Biophys. J.* 67(6):2131–33
45. Goldstein MA, Schoeter JP, Sass RL. 1990. Two structural states of the vertebrate Z band. *Electron Microsc. Rev.* 3(2):227–48
46. Gordon AM, Homsher E, Regnier M. 2000. Regulation of contraction in striated muscle. *Physiol. Rev.* 80(2):853–924
47. Gordon AM, Huxley AF, Julian FJ. 1966. The variation in isometric tension with sarcomere length in vertebrate muscle fibres. *J. Physiol.* 184(1):170–92
48. Granzier HL, Irving TC. 1995. Passive tension in cardiac muscle: contribution of collagen, titin, microtubules, and intermediate filaments. *Biophys. J.* 68(3):1027–44
49. Granzier HL, Labeit S. 2004. The giant protein titin: a major player in myocardial mechanics, signaling, and disease. *Circ. Res.* 94(3):284–95
50. Granzier HL, Labeit S. 2005. Titin and its associated proteins: the third myofilament system of the sarcomere. *Adv. Protein Chem.* 71(4):89–119

51. Granzier HL, Wang K. 1993. Passive tension and stiffness of vertebrate skeletal and insect flight muscles: the contribution of weak cross-bridges and elastic filaments. *Biophys. J.* 65(5):2141–59
52. Gruen M, Gautel M. 1999. Mutations in β-myosin S2 that cause familial hypertrophic cardiomyopathy (FHC) abolish the interaction with the regulatory domain of myosin-binding protein-C. *J. Mol. Biol.* 286(3):933–49
53. Hagopian M. 1966. The myofilament arrangement in the femoral muscle of the cockroach, *Leucophaea maderae fabricius*. *J. Cell Biol.* 28(3):545–62
54. Hamdani N, Herwig M, Linke WA. 2017. Tampering with springs: phosphorylation of titin affecting the mechanical function of cardiomyocytes. *Biophys. Rev.* 9:225–37
55. Hanson J, Huxley HE. 1953. Structural basis of the cross-striations in muscle. *Nature* 172(4377):530–32
56. Harris SP, Belknap B, Van Sciver RE, White HD, Galkin VE. 2016. C0 and C1 N-terminal Ig domains of myosin binding protein C exert different effects on thin filament activation. *PNAS* 113(6):1558–63
57. Harris SP, Lyons RG, Bezold KL. 2011. In the thick of it: HCM-causing mutations in myosin binding proteins of the thick filament. *Circ. Res.* 108(6):751–64
58. Haselgrove JC. 1975. X-ray evidence for conformational changes in the myosin filaments of vertebrate striated muscle. *J. Mol. Biol.* 92(1):113–43
59. He Z-H, Bottinelli R, Pellegrino MA, Ferenczi MA, Reggiani C. 2000. ATP consumption and efficiency of human single muscle fibers with different myosin isoform composition. *Biophys. J.* 79(2):945–61
60. Herman DS, Lam L, Taylor MRG, Wang L, Teekakirikul P, et al. 2012. Truncations of titin causing dilated cardiomyopathy. *N. Engl. J. Med.* 366(7):619–28
61. Herwig M, Kolijn D, Lódi M, Hölper S, Kovács Á, et al. 2020. Modulation of titin-based stiffness in hypertrophic cardiomyopathy via protein kinase D. *Front. Physiol.* 11:240
62. Herzberg O, James MNG. 1985. Structure of the calcium regulatory muscle protein troponin-C at 2.8 Å resolution. *Nature* 313(6004):653–59
63. Hochachka PW. 1999. The metabolic implications of intracellular circulation. *PNAS* 96(22):12233–39
64. Homsher E. 1987. Muscle enthalpy production and its relationship to actomyosin ATPase. *Annu. Rev. Physiol.* 49:673–90
65. Hoshijima M. 2006. Mechanical stress-strain sensors embedded in cardiac cytoskeleton: Z disk, titin, and associated structures. *Am. J. Physiol. Hear. Circ. Physiol.* 290(4):H1313–25
66. Houdusse A, Love ML, Dominguez R, Grabarek Z, Cohen C. 1997. Structures of four $Ca2^{+}$-bound troponin C at 2.0 Å resolution: further insights into the $Ca2^{+}$-switch in the calmodulin superfamily. *Structure* 5(12):1695–711
67. Hoyle G. 1967. Diversity of striated muscle. *Am. Zool.* 7(3):435–49
68. Huxley AF. 1957. Muscle structure and theories of contraction. *Prog. Biophys. Biophys. Chem.* 7:255–318
69. Huxley AF. 1974. Muscular contraction. *J. Physiol.* 243(1):1–43
70. Huxley AF. 1980. *Reflections on Muscle*. Liverpool, UK: Liverpool Univ. Press
71. Huxley AF, Niedergerke R. 1954. Structural changes in muscle during contraction: interference microscopy of living muscle fibres. *Nature* 173(4412):971–73
72. Huxley AF, Simmons RM. 1971. Proposed mechanism of force generation in striated muscle. *Nature* 233:533–38
73. Huxley AF, Taylor RE. 1958. Local activation of striated muscle fibres. *J. Physiol.* 144(3):426–41
74. Huxley HE. 2004. Fifty years of muscle and the sliding filament hypothesis. *Eur. J. Biochem.* 271(8):1403–15
75. Huxley HE, Brown W, Holmes KC. 1965. Constancy of axial spacings in frog sartorius muscle during contraction. *Nature* 206(991):1358
76. Huxley HE, Faruqi AR, Bordas J, Koch MHJ, Milch JR. 1980. The use of synchrotron radiation in time-resolved X-ray diffraction studies of myosin layer-line reflections during muscle contraction. *Nature* 284(5752):140–43
77. Huxley HE, Hanson J. 1954. Changes in the cross-striations of muscle during contraction and stretch and their structural interpretation. *Nature* 173(4412):973–76
78. Huxley HE, Reconditi M, Stewart A, Irving T. 2006. X-ray interference studies of crossbridge action in muscle contraction: evidence from quick releases. *J. Mol. Biol.* 363(4):743–61

79. Huxley HE, Stewart A, Sosa H, Irving T. 1994. X-ray diffraction measurements of the extensibility of actin and myosin filaments in contracting muscle. *Biophys. J.* 67(6):2411–21
80. Irving T, Wu Y, Bekyarova T, Farman GP, Fukuda N, Granzier H. 2011. Thick-filament strain and interfilament spacing in passive muscle: effect of titin-based passive tension. *Biophys. J.* 100(6):1499–508
81. Irving TC, Maughan DW. 2000. In vivo X-ray diffraction of indirect flight muscle from *Drosophila melanogaster*. *Biophys. J.* 78(5):2511–15
82. Iwamoto H. 2019. Synchrotron radiation X-ray diffraction studies on muscle: past, present, and future. *Biophys. Rev.* 11(4):547–58
83. Kaya M, Higuchi H. 2010. Nonlinear elasticity and an 8-nm working stroke of single myosin molecules in myofilaments. *Science* 329(5992):686–89
84. Kekenes-Huskey PM, Liao T, Gillette AK, Hake JE, Zhang Y, et al. 2013. Molecular and subcellular-scale modeling of nucleotide diffusion in the cardiac myofilament lattice. *Biophys. J.* 105(9):2130–40
85. Kellermayer MSZ, Smith SB, Granzier HL, Bustamante C. 1997. Folding-unfolding transitions in single titin molecules characterized with laser tweezers. *Science* 276(5315):1112–16
86. Kentish JC, McCloskey DT, Layland J, Palmer S, Leiden JM, et al. 2001. Phosphorylation of troponin I by protein kinase A accelerates relaxation and crossbridge cycle kinetics in mouse ventricular muscle. *Circ. Res.* 88(10):1059–65
87. Kinsey ST, BR Locke, Dillaman RM. 2011. Molecules in motion: influences of diffusion on metabolic structure and function in skeletal muscle. *J. Exp. Biol.* 214(2):263–74
88. Konhilas JP, Irving TC, de Tombe PP. 2002. Myofilament calcium sensitivity in skinned rat cardiac trabeculae: role of interfilament spacing. *Circ. Res.* 90:59–65
89. Koser F, Loescher C, Linke WA. 2019. Posttranslational modifications of titin from cardiac muscle: how, where, and what for? *FEBS J.* 286(12):2240–60
90. Kreutziger KL, Piroddi N, Scellini B, Tesi C, Poggesi C, Regnier M. 2008. Thin filament $Ca2^{+}$ binding properties and regulatory unit interactions alter kinetics of tension development and relaxation in rabbit skeletal muscle. *J. Physiol.* 586(Pt. 15):3683–700
91. Kushmerick MJ, Davies RE. 1969. The chemical energetics of muscle contraction. II. The chemistry, efficiency and power of maximally working sartorius muscles. *Proc. R. Soc. Lond. B* 174(1036):315–47
92. Li J, Gresham KS, Mamidi R, Doh CY, Wan X, et al. 2018. Sarcomere-based genetic enhancement of systolic cardiac function in a murine model of dilated cardiomyopathy. *Int. J. Cardiol.* 273:168–76
93. Lin BL, Li A, Mun JY, Previs MJ, Previs SB, et al. 2018. Skeletal myosin binding protein-C isoforms regulate thin filament activity in a $Ca2^{+}$-dependent manner. *Sci. Rep.* 8:2604
94. Linari M, Brunello E, Reconditi M, Fusi L, Caremani M, et al. 2015. Force generation by skeletal muscle is controlled by mechanosensing in myosin filaments. *Nature* 528(7581):276–79
95. Linari M, Caremani M, Piperio C, Brandt P, Lombardi V. 2007. Stiffness and fraction of myosin motors responsible for active force in permeabilized muscle fibers from rabbit psoas. *Biophys. J.* 92(7):2476–90
96. Linari M, Piazzesi G, Dobbie I, Koubassova NA, Reconditi M, et al. 2000. Interference fine structure and sarcomere length dependence of the axial X-ray pattern from active single muscle fibers. *PNAS* 97(13):7226–31
97. Lindstedt S, Nishikawa K. 2017. Huxley's missing filament: form and function of titin in vertebrate striated muscle. *Annu. Rev. Physiol.* 79:145–66
98. Linke WA. 2018. Titin gene and protein functions in passive and active muscle. *Annu. Rev. Physiol.* 80:389–411
99. Linke WA, Hamdani N. 2014. Gigantic business: titin properties and function through thick and thin. *Circ. Res.* 114(6):1052–68
100. Linke WA, Ivemeyer M, Mundel P, Stockmeier MR, Kolmerer B, Franzini-Armstrong C. 1998. Nature of PEVK-titin elasticity in skeletal muscle. *PNAS* 95(14):8052–57
101. Linke WA, Ivemeyer M, Olivieri N, Kolmerer B, Rüegg CJ, Labeit S. 1996. Towards a molecular understanding of the elasticity of titin. *J. Mol. Biol.* 261(1):62–71
102. Lombardi V, Piazzesi G, Reconditi M, Linari M, Lucii L, et al. 2004. X-ray diffraction studies of the contractile mechanism in single muscle fibres. *Philos. Trans. R. Soc. Lond. B* 359(1452):1883–93
103. Luther PK. 2009. The vertebrate muscle Z-disc: sarcomere anchor for structure and signalling. *J. Muscle Res. Cell Motil.* 30(5–6):171–85

104. Luther PK, Padrón R, Ritter S, Craig R, Squire JM. 2003. Heterogeneity of Z-band structure within a single muscle sarcomere: implications for sarcomere assembly. *J. Mol. Biol.* 332(1):161–69
105. Malingen SA, Asencio AM, Cass JA, Ma W, Irving TC, Daniel TL. 2020. In vivo X-ray diffraction and simultaneous EMG reveal the time course of myofilament lattice dilation and filament stretch. *J. Exp. Biol.* 223:jeb224188
106. Mann CK, Lee LC, Campbell KS, Wenk JF. 2020. Force-dependent recruitment from myosin OFF-state increases end-systolic pressure-volume relationship in left ventricle. *Biomech. Model. Mechanobiol.* 19(6):2683–92
107. Marcucci L, Washio T, Yanagida T. 2017. Titin-mediated thick filament activation, through a mechanosensing mechanism, introduces sarcomere-length dependencies in mathematical models of rat trabecula and whole ventricle. *Sci. Rep.* 7:5546
108. Marcucci L, Washio T, Yanagida T. 2019. Proposed mechanism for the length dependence of the force developed in maximally activated muscles. *Sci. Rep.* 9:1317
109. Marszalek PE, Lu H, Li H, Carrion-Vazquez M, Oberhauser AF, et al. 1999. Mechanical unfolding intermediates in titin modules. *Nature* 402(6757):100–3
110. Mártonfalvi Z, Bianco P, Linari M, Caremani M, Nagy A, et al. 2014. Low-force transitions in single titin molecules reflect a memory of contractile history. *J. Cell Sci.* 127(4):858–70
111. Maruyama K, Matsubara S, Natori R, Nonomura Y, Kimura S. 1977. Connectin, an elastic protein of muscle: characterization and function. *J. Biochem.* 82(2):317–37
112. Maruyama K, Natori R, Nonomura Y. 1976. New elastic protein from muscle. *Nature* 262(5563):58–60
113. Matsuda T, Podolsky RJ. 1986. Ordering of the myofilament lattice in muscle fibers. *J. Mol. Biol.* 189(2):361–65
114. Maughan DW, Godt RE. 1999. Parvalbumin concentration and diffusion coefficient in frog myoplasm. *J. Muscle Res. Cell Motil.* 20(2):199–209
115. McCabe KJ, Aboelkassem Y, Teitgen AE, Huber GA, McCammon JA, et al. 2020. Predicting the effects of dATP on cardiac contraction using multiscale modeling of the sarcomere. *Arch. Biochem. Biophys.* 695:108582
116. McKillop D, Geeves M. 1993. Regulation of the interaction between actin and myosin subfragment 1: evidence for three states of the thin filamen. *Biophys. J.* 65(2):693–701
117. McNamara JW, Li A, dos Remedios CG, Cooke R. 2015. The role of super-relaxed myosin in skeletal and cardiac muscle. *Biophys. Rev.* 7(1):5–14
118. McNamara JW, Sadayappan S. 2018. Skeletal myosin binding protein-C: an increasingly important regulator of striated muscle physiology. *Arch. Biochem. Biophys.* 660:121–28
119. McNamara JW, Singh RR, Sadayappan S. 2019. Cardiac myosin binding protein-C phosphorylation regulates the super-relaxed state of myosin. *PNAS* 116(24):11731–36
120. Mijailovich SM, Kayser-Herold O, Stojanovic B, Nedic D, Irving TC, Geeves MA. 2016. Three-dimensional stochastic model of actin-myosin binding in the sarcomere lattice. *J. Gen. Physiol.* 148(6):459–88
121. Millman BM. 1998. The filament lattice of striated muscle. *Physiol. Rev.* 78(2):359–91
122. Millman BM, Wakabayashi K, Racey TJ. 1983. Lateral forces in the filament lattice of vertebrate striated muscle in the rigor state. *Biophys. J.* 41(3):259–67
123. Moisescu D. 1973. Interfilament forces in striated muscle. *Bull. Math. Biol.* 35:565–75
124. Morel JE, Pinset-Härström I, Gingold MP. 1976. Muscular contraction and cytoplasmic streaming: a new general hypothesis. *J. Theor. Biol.* 62(1):17–51
125. Moss RL, Fitzsimons DP, Ralphe JC. 2015. Cardiac MyBP-C regulates the rate and force of contraction in mammalian myocardium. *Circ. Res.* 116(1):183–92
126. Mun JY, Previs MJ, Yu HY, Gulick J, Tobacman LS, et al. 2014. Myosin-binding protein C displaces tropomyosin to activate cardiac thin filaments and governs their speed by an independent mechanism. *PNAS* 111(6):2170–75
127. Nag S, Sommese RF, Ujfalusi Z, Combs A, Langer S, et al. 2015. Contractility parameters of human β-cardiac myosin with the hypertrophic cardiomyopathy mutation R403Q show loss of motor function. *Sci. Adv.* 1(9):e1500511

128. Nag S, Trivedi DV, Sarkar SS, Adhikari AS, Sunitha MS, et al. 2017. The myosin mesa and the basis of hypercontractility caused by hypertrophic cardiomyopathy mutations. *Nat. Struct. Mol. Biol.* 24(6):525–33
129. Needham DM. 1950. Myosin and adenosinetriphosphate in relation to muscle contraction. *Biochim. Biophys. Acta* 4:42–49
130. Nishikawa KC, Monroy JA, Uyeno TE, Yeo SH, Pai DK, Lindstedt SL. 2012. Is titin a "winding filament"? A new twist on muscle contraction. *Proc. R. Soc. B* 279(1730):981–90
131. Osborne MP. 1967. Supercontraction in the muscles of the blowfly larva: an ultrastructural study. *J. Insect Physiol.* 13(10):1471–82
132. Palmer BM, Swank DM, Miller MS, Tanner BCW, Meyer M, LeWinter MM. 2020. Enhancing diastolic function by strain-dependent detachment of cardiac myosin crossbridges. *J. Gen. Physiol.* 152(4):e201912484
133. Papadopoulos S, Endeward V, Revesz-Walker B, Jurgens KD, Gros G. 2001. Radial and longitudinal diffusion of myoglobin in single living heart and skeletal muscle cells. *PNAS* 98(10):5904–9
134. Pertici I, Caremani M, Reconditi M. 2019. A mechanical model of the half-sarcomere which includes the contribution of titin. *J. Muscle Res. Cell Motil.* 40(1):29–41
135. Perz-Edwards RJ, Reedy MK. 2011. Electron microscopy and X-ray diffraction evidence for two Z-band structural states. *Biophys. J.* 101(3):709–17
136. Piazzesi G, Caremani M, Linari M, Reconditi M, Lombardi V. 2018. Thick filament mechano-sensing in skeletal and cardiac muscles: a common mechanism able to adapt the energetic cost of the contraction to the task. *Front. Physiol.* 9:736
137. Piazzesi G, Lucii L, Lombardi V. 2002. The size and the speed of the working stroke of muscle myosin and its dependence on the force. *J. Physiol.* 545(1):145–51
138. Piazzesi G, Reconditi M, Linari M, Lucii L, Bianco P, et al. 2007. Skeletal muscle performance determined by modulation of number of myosin motors rather than motor force or stroke size. *Cell* 131(4):784–95
139. Piazzesi G, Reconditi M, Linari M, Lucii L, Sun Y-B, et al. 2002. Mechanism of force generation by myosin heads in skeletal muscle. *Nature* 415(6872):659–62
140. Pinzauti F, Pertici I, Reconditi M, Narayanan T, Stienen GJM, et al. 2018. The force and stiffness of myosin motors in the isometric twitch of a cardiac trabecula and the effect of the extracellular calcium concentration. *J. Physiol.* 596(13):2581–96
141. Powers JD, Bianco P, Pertici I, Reconditi M, Lombardi V, Piazzesi G. 2020. Contracting striated muscle has a dynamic I-band spring with an undamped stiffness 100 times larger than the passive stiffness. *J. Physiol.* 598(2):331–45
142. Powers JD, Williams CD, Regnier M, Daniel TL. 2018. A spatially explicit model shows how titin stiffness modulates muscle mechanics and energetics. *Integr. Comp. Biol.* 58(2):186–93
143. Powers JD, Yuan C-C, McCabe KJ, Murray JD, Childers MC, et al. 2019. Cardiac myosin activation with 2-deoxy-ATP via increased electrostatic interactions with actin. *PNAS* 116(23):11502–7
144. Previs MJ, Prosser BL, Mun JY, Previs SB, Gulick J, et al. 2015. Myosin-binding protein C corrects an intrinsic inhomogeneity in cardiac excitation-contraction coupling. *Sci. Adv.* 1(1):e1400205
145. Pyle WG, Solaro RJ. 2004. At the crossroads of myocardial signaling. *Circ. Res.* 94(3):296–305
146. Razumova MV, Bezold KL, Tu A-Y, Regnier M, Harris SP. 2008. Contribution of the myosin binding protein C motif to functional effects in permeabilized rat trabeculae. *J. Gen. Physiol.* 132(5):575–85
147. Razumova MV, Bukatina AE, Campbell KB. 2000. Different myofilament nearest-neighbor interactions have distinctive effects on contractile behavior. *Biophys. J.* 78(6):3120–37
148. Razumova MV, Shaffer JF, Tu AY, Flint GV, Regnier M, Harris SP. 2006. Effects of the N-terminal domains of myosin binding protein-C in an in vitro motility assay: evidence for long-lived cross-bridges. *J. Biol. Chem.* 281(47):35846–54
149. Reconditi M. 2006. Recent improvements in small angle X-ray diffraction for the study of muscle physiology. *Rep. Prog. Phys.* 69(10):2709–59
150. Reconditi M, Brunello E, Linari M, Bianco P, Narayanan T, et al. 2011. Motion of myosin head domains during activation and force development in skeletal muscle. *PNAS* 108(17):7236–40

151. Reconditi M, Caremani M, Pinzauti F, Powers JD, Narayanan T, et al. 2017. Myosin filament activation in the heart is tuned to the mechanical task. *PNAS* 114(12):3240–45
152. Reconditi M, Koubassova N, Linari M, Dobbie I, Narayanan T, et al. 2003. The conformation of myosin head domains in rigor muscle determined by X-ray interference. *Biophys. J.* 85(2):1098–110
153. Reconditi M, Linari M, Lucii L, Stewart A, Sun Y-B, et al. 2004. The myosin motor in muscle generates a smaller and slower working stroke at higher load. *Nature* 428(6982):578–81
154. Regnier M, Homsher E. 1998. The effect of ATP analogs on posthydrolytic and force development steps in skinned skeletal muscle fibers. *Biophys. J.* 74(6):3059–71
155. Regnier M, Lee DM, Homsher E. 1998. ATP analogs and muscle contraction: mechanics and kinetics of nucleoside triphosphate binding and hydrolysis. *Biophys. J.* 74(6):3044–58
156. Regnier M, Rivera AJ, Wang C-K, Bates MA, Chase PB, Gordon AM. 2002. Thin filament near-neighbour regulatory unit interactions affect rabbit skeletal muscle steady-state force-$Ca2^{+}$ relations. *J. Physiol.* 540(2):485–97
157. Rief M, Gautel M, Oesterhelt F, Fernandez JM, Gaub HE. 1997. Reversible unfolding of individual titin immunoglobulin domains by AFM. *Science* 276(5315):1109–12
158. Risi C, Belknap B, Forgacs-Lonart E, Harris SP, Schröder GF, et al. 2018. N-terminal domains of cardiac myosin binding protein C cooperatively activate the thin filament. *Structure* 26(12):1604–11.e4
159. Rivas-Pardo JA, Eckels EC, Popa I, Kosuri P, Linke WA, Fernández JM. 2016. Work done by titin protein folding assists muscle contraction. *Cell Rep.* 14(6):1339–47
160. Rome E. 1968. X-ray diffraction studies of the filament lattice of striated muscle in various bathing media. *J. Mol. Biol.* 37(2):331–44
161. Rose HH. 2008. Optics of high-performance electron microscopes. *Sci. Technol. Adv. Mater.* 9(1):014107
162. Royuela M, Fraile B, Arenas MI, Paniagua R. 2000. Characterization of several invertebrate muscle cell types: a comparison with vertebrate muscles. *Microsc. Res. Tech.* 48(2):107–15
163. Schoenberg M. 1980. Geometrical factors influencing muscle force development. I. The effect of filament spacing upon axial forces. *Biophys. J.* 30(1):51–67
164. Sellers JR. 2004. Fifty years of contractility research post sliding filament hypothesis. *J. Muscle Res. Cell Motil.* 25(6):475–82
165. Shaffer JF, Kensler RW, Harris SP. 2009. The myosin-binding protein C motif binds to F-actin in a phosphorylation-sensitive manner. *J. Biol. Chem.* 284(18):12318–27
166. Shear DB. 1970. Electrostatic forces in muscle contraction. *J. Theor. Biol.* 28(3):531–46
167. Shih Y-H, Dvornikov AV, Zhu P, Ma X, Kim M, et al. 2016. Exon- and contraction-dependent functions of titin in sarcomere assembly. *Development* 143(24):4713–22
168. Shimomura T, Iwamoto H, Vo Doan TT, Ishiwata S, Sato H, Suzuki M. 2016. A beetle flight muscle displays leg muscle microstructure. *Biophys. J.* 111(6):1295–303
169. Shorten PR, Sneyd J. 2009. A mathematical analysis of obstructed diffusion within skeletal muscle. *Biophys. J.* 96(12):4764–78
170. Sia SK, Li MX, Spyracopoulos L, Gagné SM, Liu W, et al. 1997. Structure of cardiac muscle troponin C unexpectedly reveals a closed regulatory domain. *J. Biol. Chem.* 272(29):18216–21
171. Smith DA. 2014. Electrostatic forces or structural scaffolding: What stabilizes the lattice spacing of relaxed skinned muscle fibers? *J. Theor. Biol.* 355:53–60
172. Smith L, Tainter C, Regnier M, Martyn DA. 2009. Cooperative cross-bridge activation of thin filaments contributes to the Frank-Starling mechanism in cardiac muscle. *Biophys. J.* 96(9):3692–702
173. Smith NP, Barclay CJ, Loiselle DS. 2005. The efficiency of muscle contraction. *Prog. Biophys. Mol. Biol.* 88(1):1–58
174. Solaro RJ, Rosevear P, Kobayashi T. 2008. The unique functions of cardiac troponin I in the control of cardiac muscle contraction and relaxation. *Biochem. Biophys. Res. Commun.* 369(1):82–87
175. Spudich JA. 2001. The myosin swinging cross-bridge model. *Nat. Rev. Mol. Cell Biol.* 2(5):387–92
176. Spudich JA. 2014. Hypertrophic and dilated cardiomyopathy: Four decades of basic research on muscle lead to potential therapeutic approaches to these devastating genetic diseases. *Biophys. J.* 106(6):1236–49
177. Spudich JA. 2015. The myosin mesa and a possible unifying hypothesis for the molecular basis of human hypertrophic cardiomyopathy. *Biochem. Soc. Trans.* 43(1):64–72

178. Squire J. 1981. *The Structural Basis of Muscular Contraction*. New York: Plenum Press
179. Squire JM. 2016. Muscle contraction: sliding filament history, sarcomere dynamics and the two Huxleys. *Glob. Cardiol. Sci. Pract.* 2016(2):e201611
180. Squire JM, Knupp C. 2005. X-ray diffraction studies of muscle and the crossbridge cycle. *Adv. Protein Chem.* 71(4):195–255
181. Stelzer JE, Dunning SB, Moss RL. 2006. Ablation of cardiac myosin-binding protein-C accelerates stretch activation in murine skinned myocardium. *Circ. Res.* 98(9):1212–18
182. Sugi H, Iwamoto H, Akimoto T, Kishi H. 2003. High mechanical efficiency of the cross-bridge power-stroke in skeletal muscle. *J. Exp. Biol.* 206(7):1201–6
183. Takada F, Woude DLV, Tong H-Q, Thompson TG, Watkins SC, et al. 2001. Myozenin: an α-actinin- and γ-filamin-binding protein of skeletal muscle Z lines. *PNAS* 98(4):1595–600
184. Tanner BCW, Daniel TL, Regnier M. 2007. Sarcomere lattice geometry influences cooperative myosin binding in muscle. *PLOS Comput. Biol.* 3(7):e115
185. Tanner BCW, Daniel TL, Regnier M. 2012. Filament compliance influences cooperative activation of thin filaments and the dynamics of force production in skeletal muscle. *PLOS Comput. Biol.* 8(5):e1002506
186. Tanner BCW, Regnier M, Daniel TL. 2008. A spatially explicit model of muscle contraction explains a relationship between activation phase, power and ATP utilization in insect flight. *J. Exp. Biol.* 211(Pt. 2):180–86
187. Tidball JG, Daniel TL. 1986. Myotendinous junctions of tonic muscle cells: structure and loading. *Cell Tissue Res.* 245(2):315–22
188. Tobacman LS. 1996. Thin filament-mediated regulation of cardiac contraction. *Annu. Rev. Physiol.* 58:447–81
189. Tonino P, Kiss B, Strom J, Methawasin M, Smith JE, et al. 2017. The giant protein titin regulates the length of the striated muscle thick filament. *Nat. Commun.* 8:1041
190. Tregear RT, Squire JM. 1973. Myosin content and filament structure in smooth and striated muscle. *J. Mol. Biol.* 77(2):279–90
191. Tskhovrebova L, Trinick J. 2012. Making muscle elastic: the structural basis of myomesin stretching. *PLOS Biol.* 10(2):e1001264
192. Tune TC, Ma W, Irving T, Sponberg S. 2020. Nanometer-scale structure differences in the myofilament lattice spacing of two cockroach leg muscles correspond to their different functions. *J. Exp. Biol.* 223(9):jeb212829
193. Tyska MJ, Hayes E, Giewat M, Seidman CE, Seidman JG, Warshaw DM. 2000. Single-molecule mechanics of R403Q cardiac myosin isolated from the mouse model of familial hypertrophic cardiomyopathy. *Circ. Res.* 86(7):737–44
194. Wakabayashi K, Sugimoto Y, Tanaka H, Ueno Y, Takezawa Y, Amemiya Y. 1994. X-ray diffraction evidence for the extensibility of actin and myosin filaments during muscle contraction. *Biophys. J.* 67(6):2422–35
195. Wang K, McClure J, Tu A. 1979. Titin: major myofibrillar components of striated muscle. *PNAS* 76(8):3698–702
196. Wang YP, Fuchs F. 1994. Length, force, and Ca(2$^+$)-troponin C affinity in cardiac and slow skeletal muscle. *Am. J. Physiol.* 266(4):C1077–82
197. Warren CM, Kobayashi T, Solaro RJ. 2009. Sites of intra- and intermolecular cross-linking of the N-terminal extension of troponin I in human cardiac whole troponin complex. *J. Biol. Chem.* 284(21):14258–66
198. Williams CD, Regnier M, Daniel TL. 2010. Axial and radial forces of cross-bridges depend on lattice spacing. *PLOS Comput. Biol.* 6(12):e1001018
199. Williams CD, Regnier M, Daniel TL. 2012. Elastic energy storage and radial forces in the myofilament lattice depend on sarcomere length. *PLOS Comput. Biol.* 8(11):e1002770
200. Williams CD, Salcedo MK, Irving TC, Regnier M, Daniel TL. 2013. The length-tension curve in muscle depends on lattice spacing. *Proc. R. Soc. B.* 280(1766):20130697
201. Winkelmann DA, Forgacs E, Miller MT, Stock AM. 2015. Structural basis for drug-induced allosteric changes to human β-cardiac myosin motor activity. *Nat. Commun.* 6:7974

202. Woodhead JL, Zhao FQ, Craig R, Egelman EH, Alamo L, Padrón R. 2005. Atomic model of a myosin filament in the relaxed state. *Nature* 436(7054):1195–99
203. Xu C, Craig R, Tobacman L, Horowitz R, Lehman W. 1999. Tropomyosin positions in regulated thin filaments revealed by cryoelectron microscopy. *Biophys. J.* 77(2):985–92
204. Yotti R, Seidman CE, Seidman JG. 2019. Advances in the genetic basis and pathogenesis of sarcomere cardiomyopathies. *Annu. Rev. Genomics Hum. Genet.* 20:129–53
205. Young P. 1998. Molecular structure of the sarcomeric Z-disk: two types of titin interactions lead to an asymmetrical sorting of alpha-actinin. *EMBO J.* 17(6):1614–24
206. Zaunbrecher RJ, Abel AN, Beussman K, Leonard A, von Frieling-Salewsky M, et al. 2019. Cronos titin is expressed in human cardiomyocytes and necessary for normal sarcomere function. *Circulation* 140(20):1647–60
207. Zou J, Tran D, Baalbaki M, Tang LF, Poon A, et al. 2015. An internal promoter underlies the difference in disease severity between N- and C-terminal truncation mutations of titin in zebrafish. *eLife* 4:e09406